Tréhu, A.M., Bohrmann, G., Torres, M.E., and Colwell, F.S. (Eds.)
Proceedings of the Ocean Drilling Program, Scientific Results Volume 204

17. Data Report: Acetate and Hydrogen Concentrations in Pore Fluids Associated with a Large Gas Hydrate Reservoir, Southern Hydrate Ridge, offshore Oregon, USA[1]

Thomas D. Lorenson,[2] Frederick S. Colwell,[3] Mark Delwiche,[3] and Jennifer A. Dougherty[2]

ABSTRACT

Acetate and hydrogen concentrations in pore fluids were measured in samples taken at seven sites from southern Hydrate Ridge (SHR) offshore Oregon, USA. Acetate concentrations ranged from 3.17 to 2515 µM. The maximum acetate concentrations occurred at Site 1251, which was drilled on a slope basin to the east of SHR at depths just above the bottom-simulating reflector (BSR) that marks the boundary of gas hydrate stability. Acetate maxima and localized high acetate concentrations occurred at the BSR at all sites and frequently corresponded with areas of gas hydrate accumulation, suggesting an empirical relationship. Acetate concentrations were typically at a minimum near the seafloor and above the sulfate/methane interface, where sulfate-reducing bacteria may consume acetate. Hydrogen concentrations in pressure core samples ranged from 16.45 to 1036 parts per million by volume (ppmv). In some cases, hydrogen and acetate concentrations were elevated concurrently, suggesting a positive correlation. However, sampling of hydrogen was limited in comparison to acetate, so any relationships between the two analytes, if present, were difficult to discern.

[1]Lorenson, T.D., Colwell, F.S., Delwiche, M., and Dougherty, J.A., 2006. Data report: Acetate and hydrogen concentrations in pore fluids associated with a large gas hydrate reservoir, southern Hydrate Ridge, offshore Oregon, USA. *In* Tréhu, A.M., Bohrmann, G., Torres, M.E., and Colwell, F.S. (Eds.), *Proc. ODP, Sci. Results,* 204, 1–20 [Online]. Available from World Wide Web: <http://www-odp.tamu.edu/publications/204_SR/VOLUME/CHAPTERS/126.PDF>. [Cited YYYY-MM-DD]
[2]U.S. Geological Survey 345 Middlefield Road, Menlo Park CA 94025, USA. Correspondence author: **tlorenson@usgs.gov**
[3]Idaho National Laboratory, 2525 North Fremont Avenue, Idaho Falls ID 83415, USA.
Present address: 104 COAS Admin Building, College of Oceanic and Atmospheric Sciences, Oregon State University, Corvallis OR 97331-5503, USA.

Initial receipt: 16 May 2005
Acceptance: 21 December 2005
Web publication: 11 September 2006
Ms 204SR-126

INTRODUCTION

Acetate and hydrogen are common products of microbial fermentation and chemical pyrolysis of organic matter. They are also common energy sources for microbial respiration reactions. Thus, these molecules are expected to be key intermediates in subsurface microbial activities. Methane, a primary product of acetoclastic methanogenesis or carbonate reduction, coexists in the pore water or as gas hydrate in close proximity to methanogens.

Globally, much of the methane found in seafloor hydrates has a light stable isotope signature for carbon that suggests it was produced by microbial (i.e., methanogenic) activity (Kvenvolden, 1995). Methanogens, members of the domain Archaea, are important contributors to the oxidation of organic matter. Despite the difficulty in detecting methanogens in sediments that contain hydrates (Reed et al., 2002; Inagaki et al., 2003), it is expected that their presence is key to the formation of large methane hydrate deposits that possess biogenic methane.

Methanogens are found in numerous anoxic environments on Earth. They depend upon aerobic and anaerobic microbial communities to oxidize more complex forms of organic materials into the small organic molecules that they can use (Fenchel and Blackburn, 1979). Many methanogens also use hydrogen as a source of energy. Hydrogen can be generated from biological or abiological processes (Morita, 2000) and may serve as a fundamental means of survival for many organisms in the subsurface. In subseafloor environments, acetate and hydrogen are two of the most likely sources of energy for methanogens (Whiticar et al., 1986). Acetoclastic methanogens have been suggested as key contributors to the methane that exists within hydrates on Blake Ridge, one of the most intensively studied hydrate sites in the world (Wellsbury et al., 1997). At Blake Ridge, Wellsbury et al. (1997) detected high concentrations of acetate that corresponded to high rates of acetoclastic methanogenesis as measured in the laboratory.

The concentration of energy-yielding compounds in microbial habitats is a critical element for estimating the rate of microbial activity in these environments. Acetate concentrations in anoxic marine sediments are typically low and maintained at those low levels because of microbial activity. In shallow Blake Ridge sediments, acetate concentrations in pore waters remained close to ~7 µM through the uppermost 80 m of sediments (Wellsbury et al., 1997). However, as depth increased in this location, higher values were detected (up to 15,000 µM).

Acetate concentrations have been measured on a few occasions in deep marine boreholes such as Ocean Drilling Program (ODP) Leg 164 on Blake Ridge, (Egeberg and Barth, 1998), Leg 177 in the Southern Ocean (Wellsbury et al., 2001), Leg 201 on the Peruvian continental margin (Shipboard Scientific Party, 2002), and the present study. Only the Southern Ocean study area did not have gas hydrate deposits associated with some of the drilling locations. Total bacterial abundances have been measured in sediments for each of these four legs, and, more specifically, during Leg 204 methanogenic archaea were counted by Boyd (2005).

Hydrogen concentrations in marine sediments vary according to the terminal electron-accepting process (TEAP) that dominates in a particular location in the sediments. For example, in Cape Lookout bight sediments, hydrogen concentrations ranged from a low of 0.031 nM, where

nitrate reduction was the dominant TEAP, to a high of 133 nM, where acetogenesis was the dominant TEAP (Hoehler et al., 1998).

Hydrogen concentrations have been previously measured during Leg 201, where they reached a maximum concentration of 102 nM at Site 1231 (Shipboard Scientific Party, 2002). At Site 1230, where gas hydrates were recovered from multiple depths ranging from 123 to 200 meters below seafloor (mbsf), hydrogen concentrations reached a maximum of 1.45 nM; however, the sample density was too low to derive a correlation of hydrogen concentrations with intervals bearing gas hydrate.

LOCATION

Hydrate Ridge is a 25-km-long, 15-km-wide accretionary ridge located on the continental margin ~80 km west of Newport, Oregon (Fig. F1). A widespread bottom-simulating reflector (BSR), numerous seafloor gas vents, outcrops and subcrops of gas hydrate, authigenic carbonates, and chemosynthetic organisms characterize the area (Tréhu, Bohrmann, Rack, Torres, et al., 2003). During Leg 204, nine sites (1244–1252) were drilled and cored on southern Hydrate Ridge (SHR). From seven of these sites, highlighted in red on Figure F1, we collected the samples reported in this study. Detailed descriptions of the geologic and biologic setting can be found in the Leg 204 *Initial Reports* volume (Tréhu, Bohrmann, Rack, Torres, et al., 2003) and references therein.

F1. Location map and tectonic setting of Hydrate Ridge, p. 9.

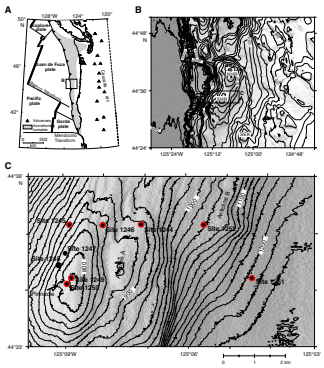

SAMPLING METHODS AND HANDLING

Gas samples for hydrogen analyses were retrieved from the pressure core sampling (PCS) device. The workings and deployment of this device are described in detail in Tréhu, Bohrmann, Rack, Torres, et al. (2003). The use of the PCS allowed for the collection of the best possible in situ gas samples.

The PCS cores were degassed for periods of 450–2999 min onboard the ship (Milkov et al., 2003). Evolved gas was collected in a series of sample increments by allowing gas to bubble through a water bath and captured in an inverted plastic graduated cylinder. Gas was removed from the graduated cylinder by a syringe. Gas aliquots were then placed into 30-mL serum vials by water displacement. The vials were sealed and stored at 4°C until analysis.

Samples destined for acetate concentration measurement were collected in conjunction with other interstitial water (IW) samples. The majority of shipboard IW samples were obtained on 5- to 20-cm-long whole-round cores that were cut according to two general procedures described in Tréhu, Bohrmann, Rack, Torres, et al. (2003). Uncontaminated sediment (~150–300 cm^3) was placed into a titanium squeezer (modified after the stainless steel squeezer of Manheim and Sayles [1974]), filtered through a 0.45-µm Gelman polysulfone disposable filter, and collected in a plastic syringe over the course of 20–40 min. The fluids were then filtered again through a 0.2-µm inline filter, and ~3-mL subsamples of this pore water were stored in glass vials for analyses of dissolved volatile fatty acids. The samples were kept frozen until analyzed.

ANALYTICAL METHODS

For hydrogen analyses, we used a 3800 Varian gas chromatograph equipped with three separate sample loops, three sets of columns, and three distinct detectors for gas analysis. Gas samples were withdrawn from the serum vial by piercing the solid rubber seal with a needle attached to a gas-tight glass syringe. The gas chromatograph was configured with argon as the carrier gas, an evacuated 1-mL sample loop, and a thermal conductivity detector (TCD). Helium and H_2 are detected with the most sensitivity with detection limits of 2 parts per million (ppm). Methane is detected in concentrations above 20 parts per million by volume (ppmv). The TCD sample arm is controlled by a Type 4 electronic flow controller and is fed by a sample loop that uses two columns in series, a Hayesep R column (4 ft × ⅛ in, 80–100 mesh, silco steel), followed by a Molsieve 5A column (10 ft × ⅛ in, 60–80 mesh, silco steel). Run conditions are isothermal at 50°C at 21 mL/min.

Measurements on replicate sediment samples generally have a precision of ~5%. Accuracy of the chromatographic analysis is estimated to be 2% based on comparison of standards, and the precision is ~2%.

Acetate ion concentration of extracted pore water was determined by high-performance liquid chromotagraphy using a Shimadzu VP series chromatograph with an ultraviolet-visual light detector (SVP-10AVP) set at 210 nm. IW samples were allowed to thaw at room temperature, and ~1 mL was transferred to autosampler vials for immediate analyses. Acetate was separated using two columns in series (Bio-Rad Aminex HPX-87H and Hamilton PRP X300) with a 0.016-N sulfuric acid eluent flowing at 0.6 mL/min. The retention time for acetate was 25.8 min under these conditions. Detection limits of these analyses were ~3 µM. Acetate concentrations were calculated based on peak height from a five-point standard calibration curve. Measurements on replicate sediment samples generally have a precision of ~2%. Accuracy of the chromatographic analysis is estimated to be 1% based on comparison of standards, and the precision is also ~1%.

RESULTS

Acetate and hydrogen concentrations in pore fluids were measured from samples taken at seven sites from SHR. Figures **F2, F3, F4, F5, F6, F7,** and **F8** show plots of acetate ion and hydrogen concentration with depth for each site.

Acetate concentrations ranged from 3.17 to 2515 µM (Table **T1**). Acetate concentrations are typically lowest within the upper 10 mbsf, above the sulfate/methane interface (SMI), and highest at various depths downhole, suggesting that in these shallow sediments, sulfate-reducing bacteria may consume acetate.

Within the gas hydrate stability zone, there are discrete excursions to high acetate concentrations at all sites. Hydrate distribution was constrained by Tréhu et al. (2004) using a multiproxy approach; however, given the spatial variability of the various proxies, here we correlate the acetate concentration with gas hydrate abundance in pore space primarily derived from dissolved chloride anomalies indicative of hydrate presence. Both chloride and acetate data were obtained in the same IW samples at similar intervals. A comparison between the acetate maxima and the discrete spikes in chloride concentration reveals that there is a

F2. Acetate and hydrogen, Site 1244, p. 10.

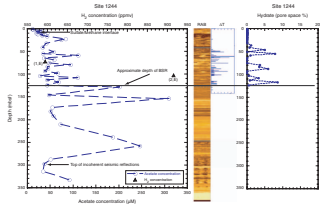

F3. Acetate, Site 1245, p. 11.

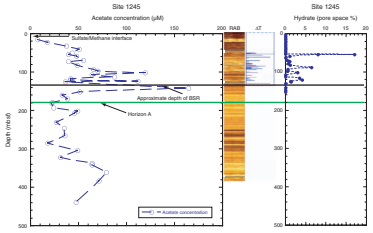

F4. Acetate, Site 1246, p. 12.

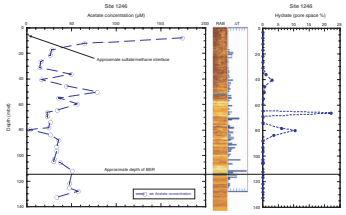

F5. Acetate and hydrogen, Site 1249, p. 13.

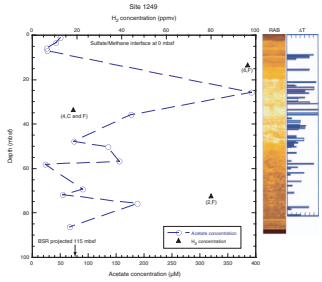

F6. Acetate and hydrogen, Site 1250, p. 14.

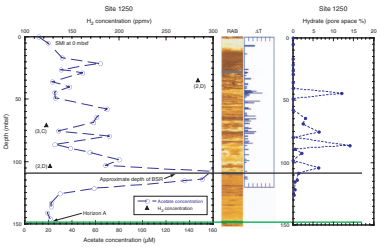

general correspondence of higher concentrations of acetate. Hydrogen concentrations were measured in too few places to make any correlations; however, the build up of both acetate and hydrogen below the SMI suggests a buildup of microbial energy sources.

Acetate concentration maxima occurred at or near the BSR at Sites 1245, 1250, and 1251, and high concentrations were also observed at Sites 1244, 1246, and 1252. It is perhaps significant that the best defined maxima at the BSR occur at Sites 1250 and 1251, where the enhanced acetate content is observed in several samples, and at Site 1251 reaches values of 2600 µM. Based on PCS data, it is apparent that there is free gas underneath the BSR at these locations, although at Site 1251 it is only a few percent of the available pore space (Tréhu, Bohrmann, Rack, Torres, et al., 2003). Hydrogen concentrations are noted by the format (number, letter) in Figures **F2, F3, F4, F5, F6, F7,** and **F8,** indicating the average concentration of that number of samples, while the letter designates the hole (e.g., 1244E). Hydrogen concentrations in PCS gases ranged from 16.45 to 1036 ppmv and are listed in Table **T2.** Hydrogen concentrations measured while degassing the PCS cannot be directly related to in situ concentration in pore water because of the sampling method; thus, the results given in ppmv should be considered as relative, semiquantitative concentrations. Hydrogen concentration measurements were attempted on ~20 headspace samples (i.e., approximately a 5-cm^3 sediment plug). For each of these samples, hydrogen concentration was below the detection limit of about 10 ppmv, corresponding to concentrations of less than ~4 nM.

In general, pore water acetate concentrations in samples from Leg 204 were high in comparison to the non-gas hydrate–bearing Southern Ocean region, which range from 0 to 110 µM (Wellsbury et al., 2001). High acetate concentrations in this region were associated with the presence of localized diatom-rich laminae in the sediments at Site 1093 (Gersonde, Hodell, Blum, et al., 1999). In contrast, data from Leg 164 showed acetate concentrations exceeding 15,000 µM at ~700 mbsf in Site 997 (Egeberg and Barth, 1998; Wellsbury et al., 2000). These sediments were recovered from biogeochemically active zones (Wellsbury et al., 2000) with extensive gas hydrate deposits (Dickens et al., 1997). Drilling conducted during Leg 201 also showed high acetate concentrations at the Peru slope hydrate site (Site 1230). Here the acetate concentration reached 230 µM at 145 mbsf and corresponded to the presence of gas hydrate at 142 mbsf (Shipboard Scientific Party, 2002). The results from each of these legs suggest that the high acetate concentrations in the pore waters of gas-hydrated sediments or sediments containing unusually high concentrations of methane are unique and not the general situation in deep marine sediments. A similar conclusion was reached by Wellsbury et al. (2001).

Acetogenesis rates may increase with rising temperatures, resulting in an increase in acetate concentrations with increasing depth. Such an increase with depth was observed by Wellsbury et al. (1997) at Blake Ridge, offshore the southeastern Atlantic coast of the United States. They concluded that the acetate concentration buildup was indeed due to acetogenesis brought on by early diagenesis of organic matter and that the acetate helped fuel the generation of methane by methanogens utilizing acetate via the acetate fermentation pathway. A plot of Leg 204 acetate ion concentration vs. temperature (Fig. **F9**) reveals the lack of any general relationship that would suggest that acetogenesis via degradation of organic matter or early pyrolysis takes place at these sites.

F7. Acetate and hydrogen, Site 1251, p. 15.

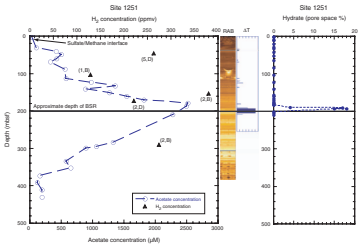

F8. Acetate, Site 1252, p. 16.

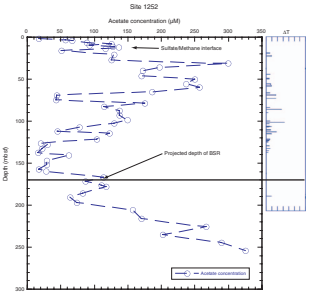

T1. Acetate in interstitial pore water, p. 18.

T2. Hydrogen, helium, and methane gas concentrations, p. 20.

F9. Leg 204 acetate ion concentration vs. temperature, p. 17.

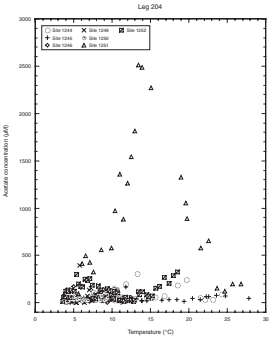

CONCLUSIONS

Acetate and hydrogen concentrations in the pore water of Leg 204 sites were elevated relative to non-gas hydrate–bearing sites where such measurements have previously been made. The maximum acetate concentrations occurred at Site 1251, an area to the east of SHR at just above the BSR, a zone of very high methane concentration. Acetate maxima or locally high concentrations of acetate occurred at the BSR at all sites, and frequently correspond with areas of gas hydrate accumulation and high methane concentrations. Hydrogen data are sparse and qualitative; however, they indicate that elevated concentrations of hydrogen exist in these sediments. It would be beneficial to allocate more samples for hydrogen analyses in future seafloor coring efforts.

ACKNOWLEDGMENTS

This research used samples provided by the Ocean Drilling Program (ODP), which is sponsored by the US National Science foundation (NSF) and participating countries under management of Joint Oceanographic Institutions (JOI), Inc. Many thanks are given to the ODP staff, crew and scientists onboard the *JOIDES Resolution* for allowing us to obtain samples from Leg 204. ODP, the National Science Foundation, the U.S. Department of Energy, and the U.S. Geological Survey funded this work. Andy Ovimette and Bill Evans provided expertise and help with hydrogen analyses.

REFERENCES

Boyd, S., 2005. Detection and quantification of methanogens in methane hydrate samples using the quantitative polymerase chain reaction (QPCR) (M.S. Thesis). Univ. Idaho, Moscow.

Dickens, G.R., Paull, C.K., Wallace, P., and the ODP Leg 164 Scientific Party, 1997. Direct measurement of in situ methane quantities in a large gas-hydrate reservoir. *Nature (London, U. K.),* 385:427–428. **doi:10.1038/385426a0**

Egeberg, P.K., and Barth, T., 1998. Contribution of dissolved organic species to the carbon and energy budgets of hydrate bearing deep sea sediments (Ocean Drilling Program Site 997 Blake Ridge). *Chem. Geol.,* 149:25–35. **doi:10.1016/S0009-2541(98)00033-3**

Fenchel, T., and Blackburn, T.H., 1979. *Bacteria and Mineral Cycling:* London (Academic Press).

Gersonde, R., Hodell, D.A., Blum, P., et al., 1999. *Proc. ODP, Init. Repts.,* 177 [CD-ROM]. Available from: Ocean Drilling Program, Texas A&M University, College Station, TX 77845-9547, U.S.A. [**HTML**]

Hoehler, T.M., Alperin, M.J., Albert, D.B., and Martens, C.S., 1998. Thermodynamic control on hydrogen concentrations in anoxic sediments. *Geochim. Cosmochim. Acta,* 62:1745–1756. **doi:10.1016/S0016-7037(98)00106-9**

Inagaki, F., Nunoura, T., Suzuki, M., Takai, K., Nealson, K.H., Horikoshi, K., Delwiche, M.E., Colwell, F., Jørgensen, B.B., and ODP Legs 201 and 204 Shipboard Parties, 2003. Microbial community structures in methane hydrate–bearing deep marine sediments from the Peru margin (ODP Leg 201) and the Cascadia margin (ODP Leg 204). *Eos, Trans. Am. Geophys. Union,* 84(46):B42C-06. (Abstract)

Kvenvolden, K.A., 1995. A review of the geochemistry of methane in natural gas hydrate. *Org. Geochem.,* 23:997–1008. **doi:10.1016/0146-6380(96)00002-2**

Manheim, F.T., and Sayles, F.L., 1974. Composition and origin of interstitial waters of marine sediments, based on deep sea drill cores. *In* Goldberg, E.D. (Ed.), *The Sea* (Vol. 5): *Marine Chemistry: The Sedimentary Cycle:* New York (Wiley), 527–568.

Milkov, A.V., Claypool, G.E., Lee, Y-J., Xu, W., Dickens, G.R., Borowski, W.S., and the ODP Leg 204 Scientific Party, 2003. In situ methane concentrations at Hydrate Ridge offshore Oregon: new constraints on the global gas hydrate inventory from an active margin. *Geology,* 31:833–836.

Morita, R.Y., 2000. Is H_2 the universal energy source for long-term survival? *Microb. Ecol.,* 38:307–320. **doi:10.1007/s002489901002**

Reed, D.W., Fujita, Y., Delwiche, M., Blackwelder, D.B., Sheridan, P.P., Uchida, T., and Colwell, F., 2002. Microbial communities from methane hydrate–bearing deep marine sediments in a forearc basin. *Appl. Environ. Microbiol.,* 68:3759–3770. **doi:10.1128/AEM.68.8.3759-3770.2002**

Shipboard Scientific Party, 2003. Leg 201 summary. *In* D'Hondt, S.L., Jørgensen, B.B., Miller, D.J., et al., *Proc. ODP, Init. Repts.,* 201: College Station TX (Ocean Drilling Program), 1–81. [**HTML**]

Shipboard Scientific Party, 2002. Leg 201 Preliminary Report. *ODP Prelim. Rpt.,* 101 [Online]. Available from World Wide Web: <**http://www-odp.tamu.edu/publications/prelim/201_prel/201PREL.PDF**>. [Cited 2005-03-15]

Tréhu, A.M., Bohrmann, G., Rack, F.R., Torres, M.E., et al., 2003. *Proc. ODP, Init. Repts.,* 204 [CD-ROM]. Available from: Ocean Drilling Program, Texas A&M University, College Station TX 77845-9547, USA. [**HTML**]

Tréhu, A.M., Long, P.E., Torres, M.E., Bohrmann, G., Rack, F.R., Collett, T.S., Goldberg, D.S., Milkov, A.V., Riedel, M., Schultheiss, P., Bangs, N.L., Barr, S.R., Borowski, W.S., Claypool, G.E., Delwiche, M.E., Dickens, G.R., Gracia, E., Guerin, G., Holland, M., Johnson, J.E., Lee, Y.-J., Liu, C.-S., Su, X., Teichert, B., Tomaru, H., Vanneste, M., Watanabe, M., and Weinberger, J.L., 2004. Three-dimensional distribution of gas

hydrate beneath southern Hydrate Ridge: constraints from ODP Leg 204. *Earth Planet. Sci. Lett.,* 222:845–862. **doi:10.1016/j.epsl.2004.03.035**

Wellsbury, P., Goodman, K., Barth, T., Cragg, B.A., Barnes, S.P., and Parkes, R.J., 1997. Deep marine biosphere fueled by increasing organic matter availability during burial and heating. *Nature (London, U. K.),* 388:573–576.

Wellsbury, P., Goodman, K., Cragg, B.A., and Parkes, R.J., 2000. The geomicrobiology of deep marine sediments from Blake Ridge containing methane hydrate (Sites 994, 995, and 997). *In* Paull, C.K., Matsumoto, R., Wallace, P.J., and Dillon, W.P. (Eds.), *Proc. ODP, Sci. Results,* 164: College Station, TX (Ocean Drilling Program), 379–391. [**HTML**]

Wellsbury, P., Mather, I.D., and Parkes, R.J., 2001. Bacterial abundances and pore-water acetate concentrations in sediments of the Southern Ocean (Sites 1088 and 1093). *In* Gersonde, R., Hodell, D.A., and Blum, P. (Eds.), *Proc. ODP, Sci. Results,* 177 [Online]. Available from World Wide Web: <**http://www-odp.tamu.edu/publications/177_SR/chap_03/chap_03.htm**>. [Cited 2005-03-15]

Whiticar, M.J., Faber, E., and Schoell, M., 1986. Biogenic methane formation in marine and freshwater environments: CO_2 reduction vs. acetate fermentation—isotope evidence. *Geochim. Cosmochim. Acta,* 50:693–709. **doi:10.1016/0016-7037(86)90346-7**

Figure F1. A. Location map and tectonic setting of Hydrate Ridge. Inset shows region of (B). **B.** Bathymetry of the Hydrate Ridge vicinity Inset shows the location of (C). SHR = southern Hydrate Ridge. NHR = northern Hydrate Ridge. SEK = Southeast Knoll. **C.** Locations of ODP Site 892 and those drilled during Leg 204. Sites where acetate and hydrogen concentrations were measured are noted in red and solid circles. Figure modified from Tréhu, Bohrmann, Rack, Torres, et al. (2003) and Shipboard Scientific Party (2003).

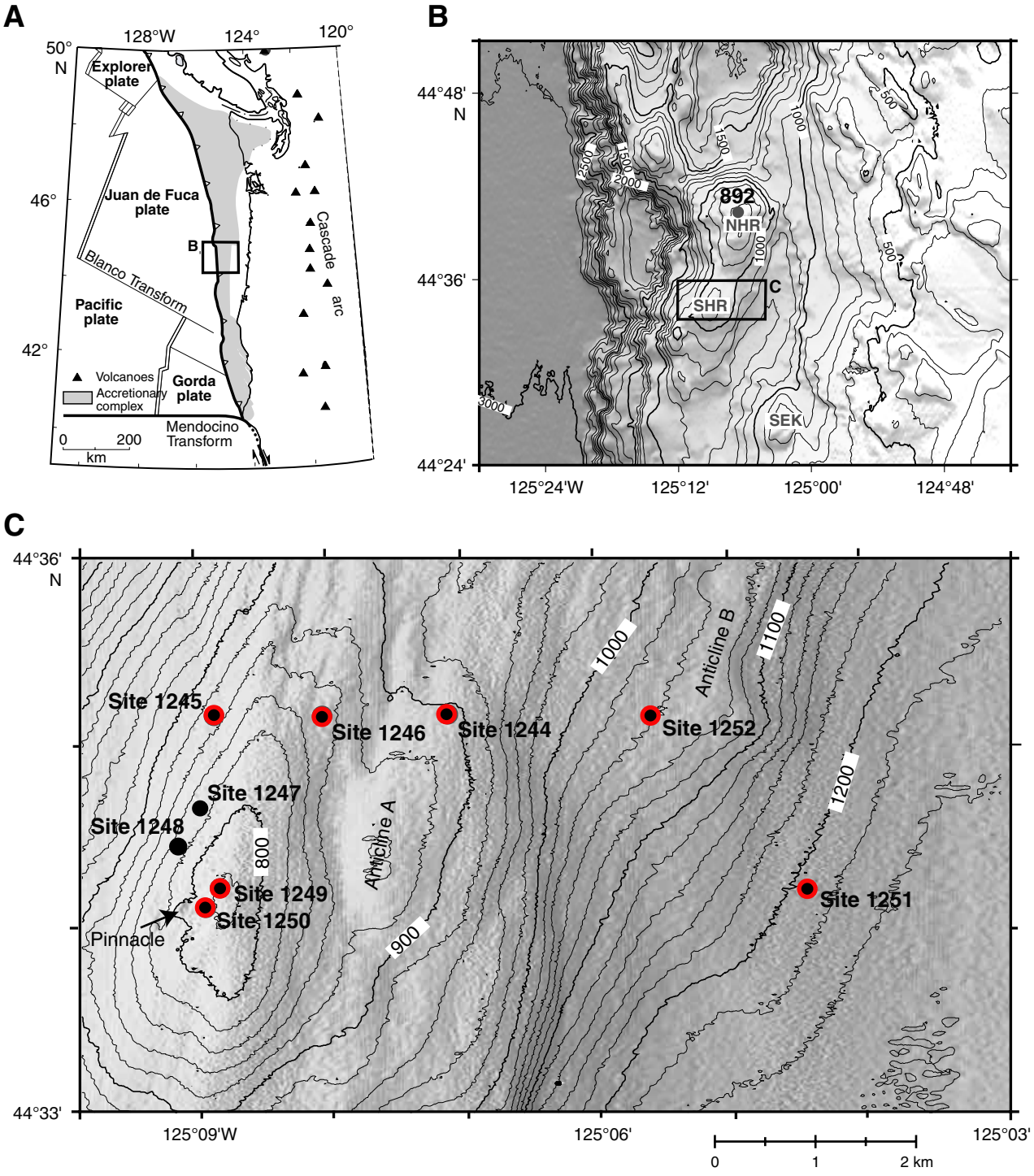

Figure F2. Plot of acetate ion and hydrogen concentration with depth for Site 1244. Hydrogen concentrations are noted by the format (number, letter) indicating the average concentration of that number of samples, while the letter designates the hole (e.g., [2,E] corresponds to Hole 1244E). The panel to the right is of the relative borehole resistivity as imaged by the resistivity-at-the-bit (RAB) tool. Lighter-colored bands represent areas of higher resistivity which are likely to be gas hydrate above the BSR. The next panel shows low-temperature anomalies recorded by infrared camera scans (blue spikes), which indicate likely areas of gas hydrate decomposition in the recovered core. The graph on the far right plots the calculated percentage of pore space occupied by gas hydrate according to Tréhu et al. (2004). ΔT = temperature change.

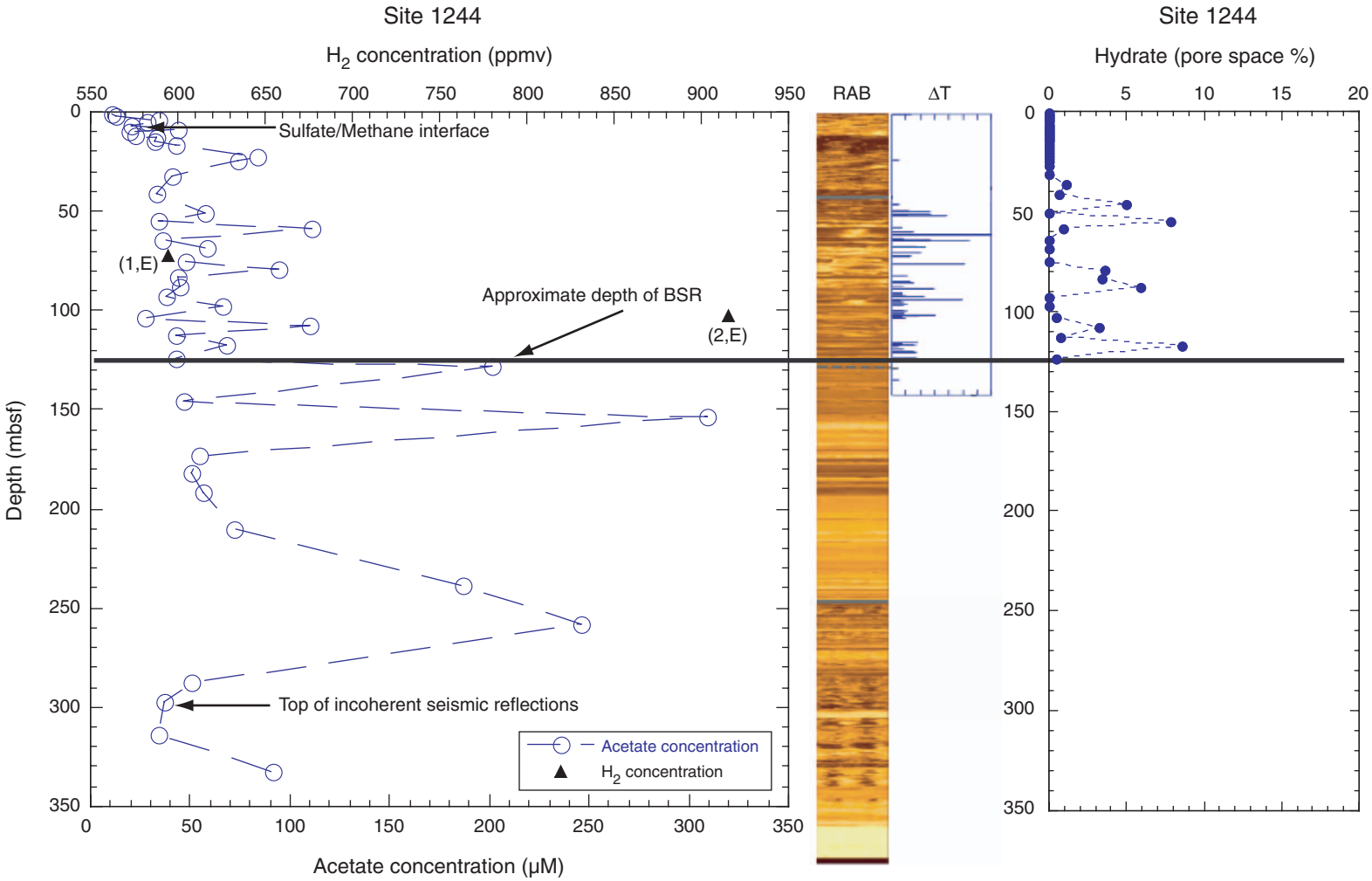

Figure F3. Plot of acetate ion concentration with depth for Site 1245. The panel to the right is of the relative borehole resistivity as imaged by the resistivity-at-the-bit (RAB) tool. Lighter-colored bands represent areas of higher resistivity which are likely to be gas hydrate above the bottom-simulating reflector (BSR). The next panel shows low-temperature anomalies recorded by infrared camera scans (blue spikes), which indicate likely areas of gas hydrate decomposition in the recovered core. The graph on the far right plots the calculated percentage of pore space occupied by gas hydrate according to Tréhu et al. (2004). ΔT = temperature change.

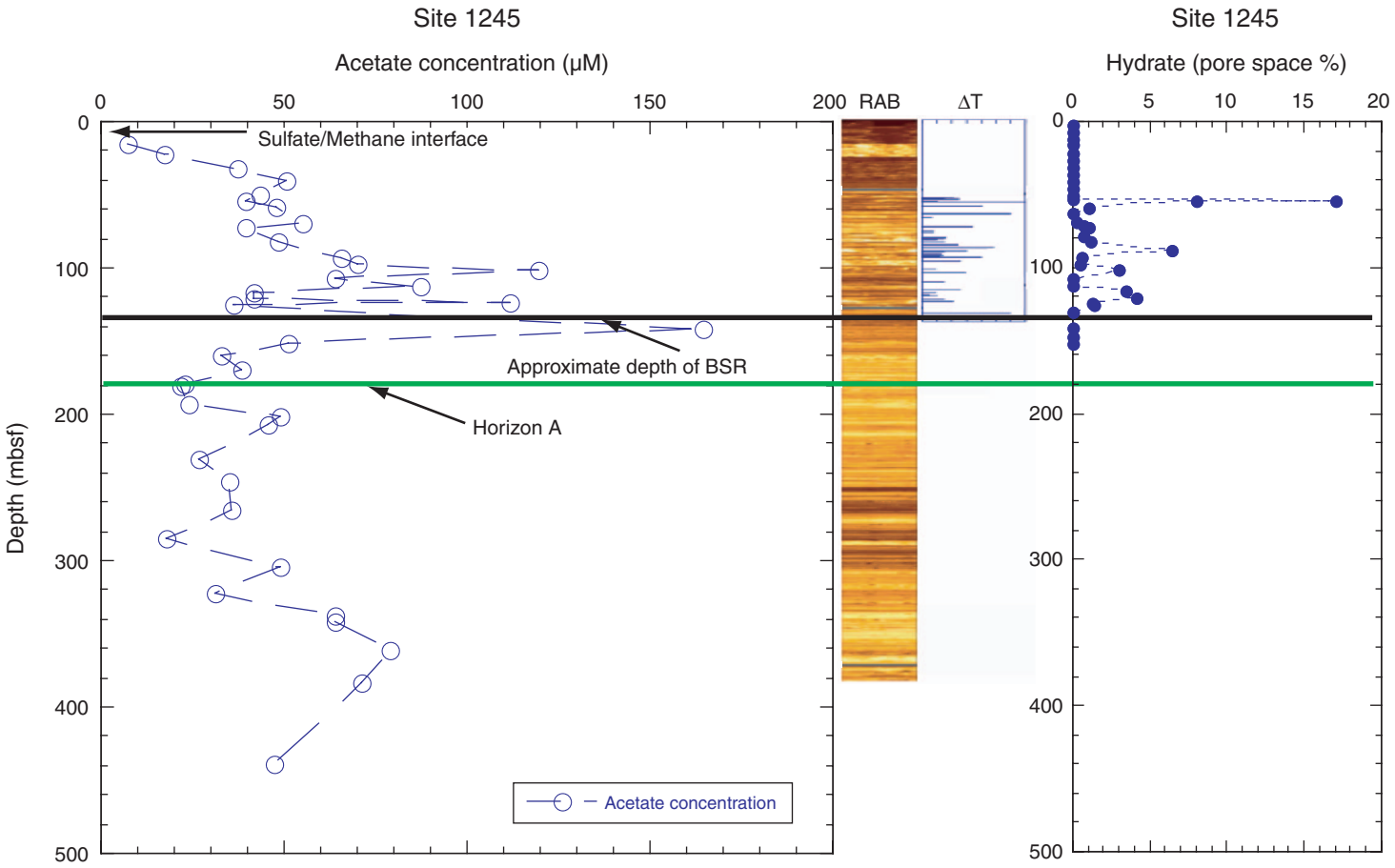

Figure F4. Plot of acetate ion concentration with depth for Site 1246. The panel to the right is of the relative borehole resistivity as imaged by the resistivity-at-the-bit (RAB) tool. Lighter-colored bands represent areas of higher resistivity which are likely to be gas hydrate above the bottom-simulating reflector (BSR). The next panel shows low-temperature anomalies recorded by infrared camera scans (blue spikes), which indicate likely areas of gas hydrate decomposition in the recovered core. The graph on the far right plots the calculated percentage of pore space occupied by gas hydrate according to Tréhu et al. (2004). ΔT = temperature change.

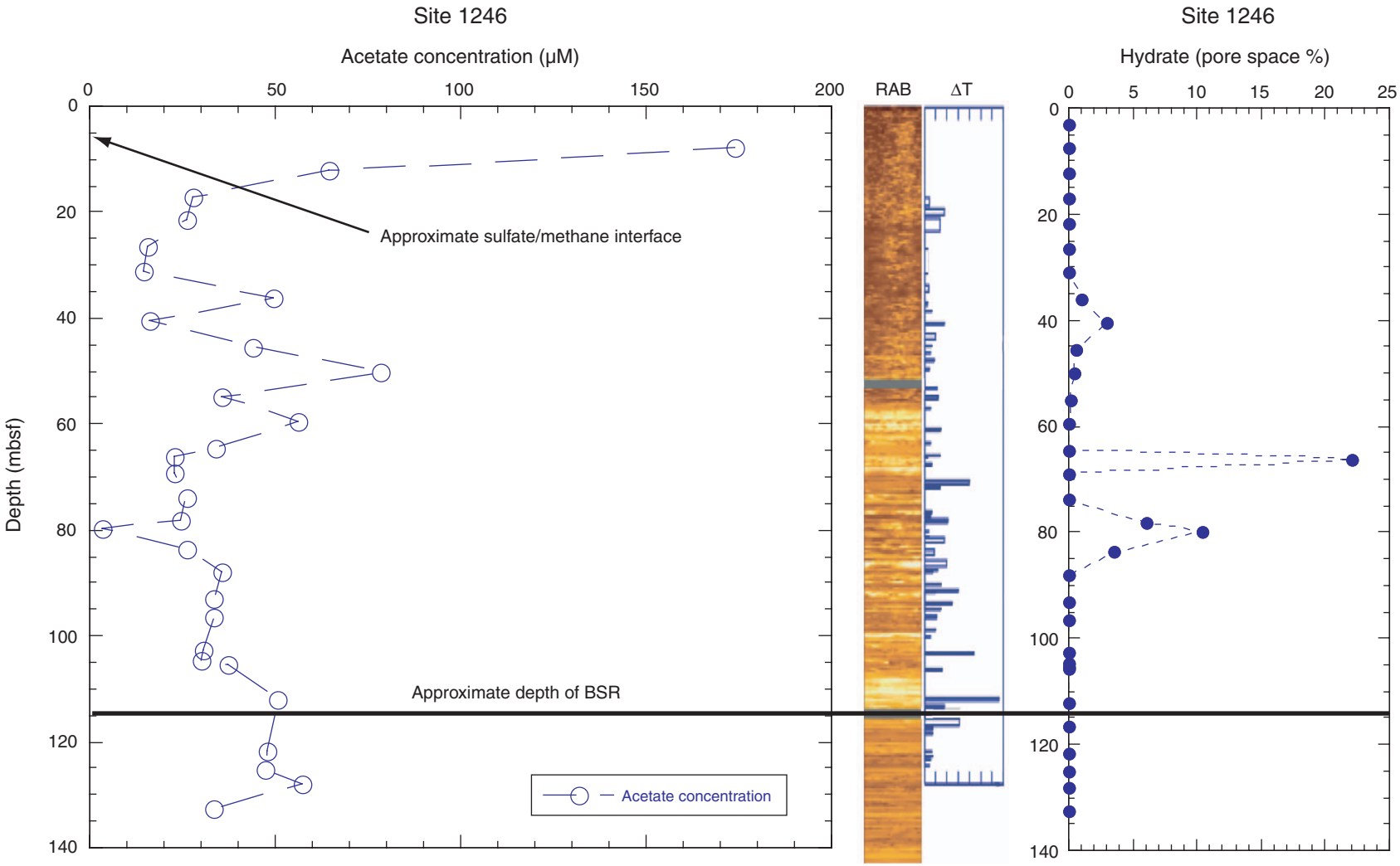

Figure F5. Plot of acetate ion and hydrogen concentration with depth for Site 1249. Hydrogen concentrations are noted by the format (number, letter) indicating the average concentration of that number of samples, while the letter designates the hole (e.g., [6,F] corresponds to Hole 1249F). The panel to the right is of the relative borehole resistivity as imaged by the resistivity-at-the-bit (RAB) tool. Lighter-colored bands represent areas of higher resistivity which are likely to be gas hydrate above the bottom-simulating reflector (BSR). The next panel shows low-temperature anomalies recorded by infrared camera scans (blue spikes), which indicate likely areas of gas hydrate decomposition in the recovered core. ΔT = temperature change.

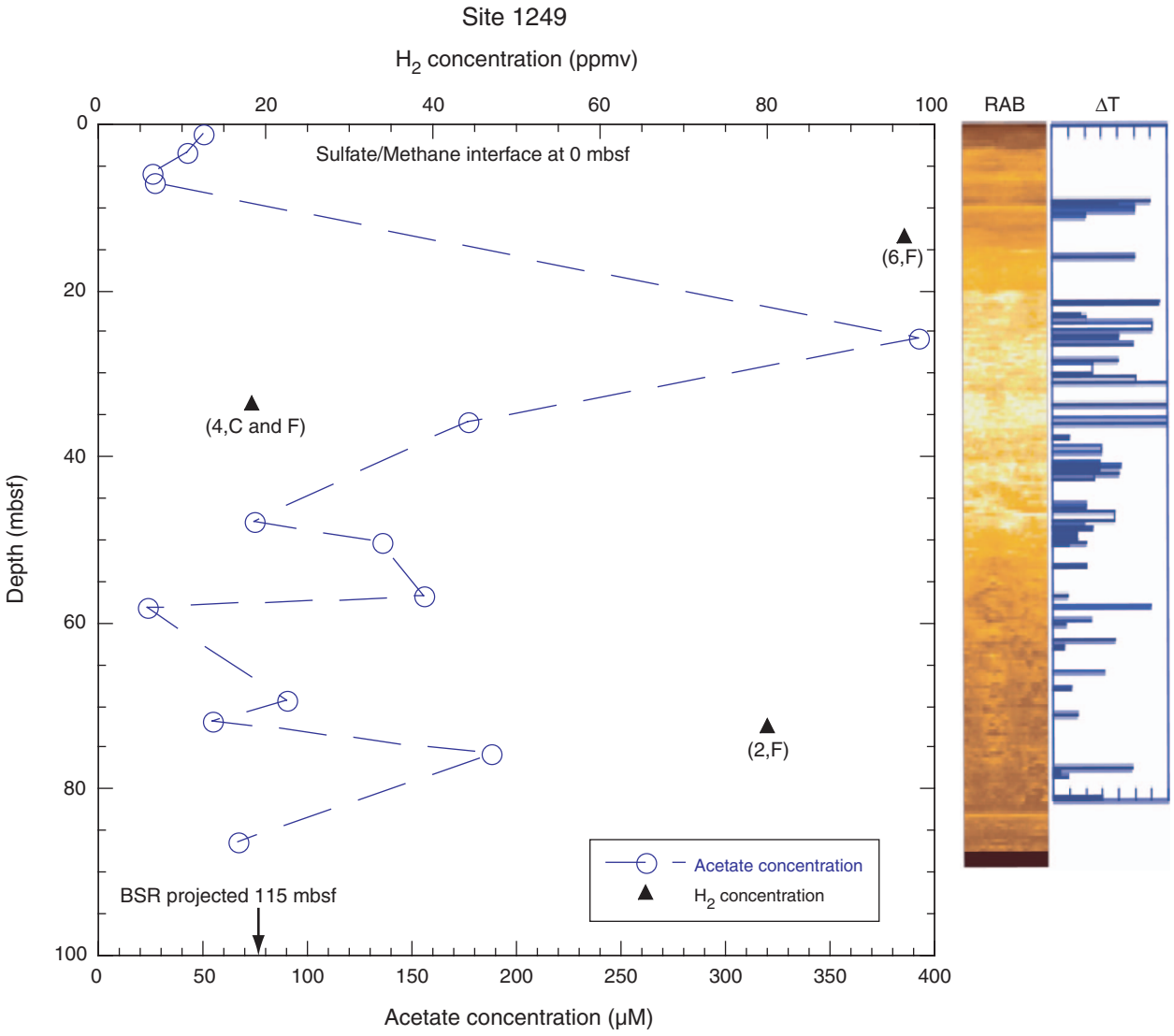

Figure F6. Plot of acetate ion and hydrogen concentration with depth for Site 1250. Hydrogen concentrations are noted by the format (number, letter) indicating the average concentration of that number of samples, while the letter designates the hole (e.g., [2,D] corresponds to Hole 1250D). The panel to the right is of the relative borehole resistivity as imaged by the resistivity-at-the-bit (RAB) tool. Lighter-colored bands represent areas of higher resistivity which are likely to be gas hydrate above the bottom-simulating reflector (BSR). The next panel shows low-temperature anomalies recorded by infrared camera scans (blue spikes), which indicate likely areas of gas hydrate decomposition in the recovered core. The graph on the far right plots the calculated percentage of pore space occupied by gas hydrate according to Tréhu et al. (2004). ΔT = temperature change. SMI = sulfate/methane interface.

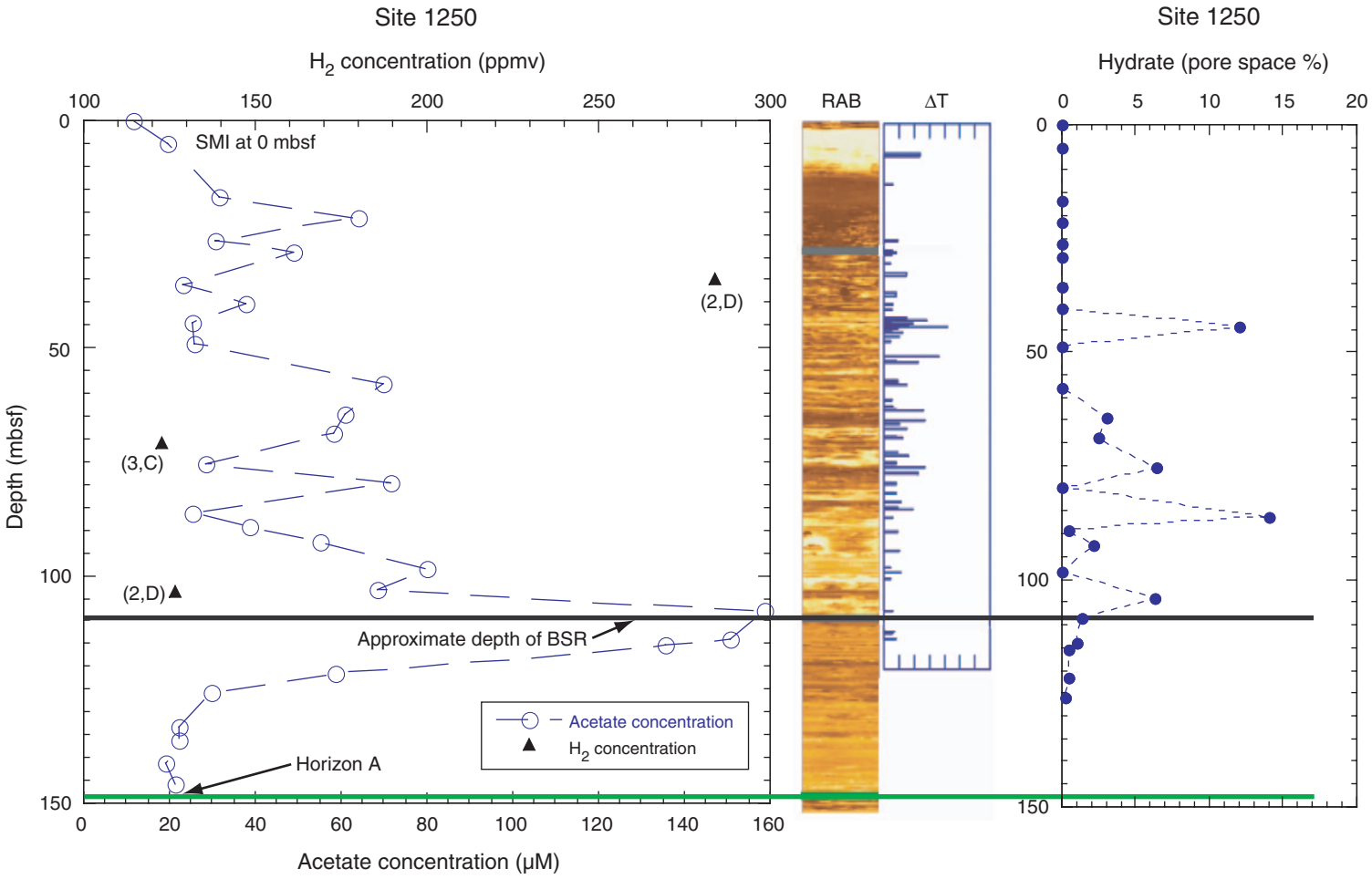

Figure F7. Plot of acetate ion and hydrogen concentration with depth for Site 1251. Hydrogen concentrations are noted by the format (number, letter) indicating the average concentration of that number of samples, while the letter designates the hole (e.g., [5,E] corresponds to Hole 1251D). The panel to the right is of the relative borehole resistivity as imaged by the resistivity-at-the-bit (RAB) tool. Lighter-colored bands represent areas of higher resistivity, which are likely to be gas hydrate above the bottom-simulating reflector (BSR). The next panel shows low-temperature anomalies recorded by infrared camera scans (blue spikes), which indicate likely areas of gas hydrate decomposition in the recovered core. The graph on the far right plots the calculated percentage of pore space occupied by gas hydrate according to Tréhu et al. (2004). ΔT = temperature change.

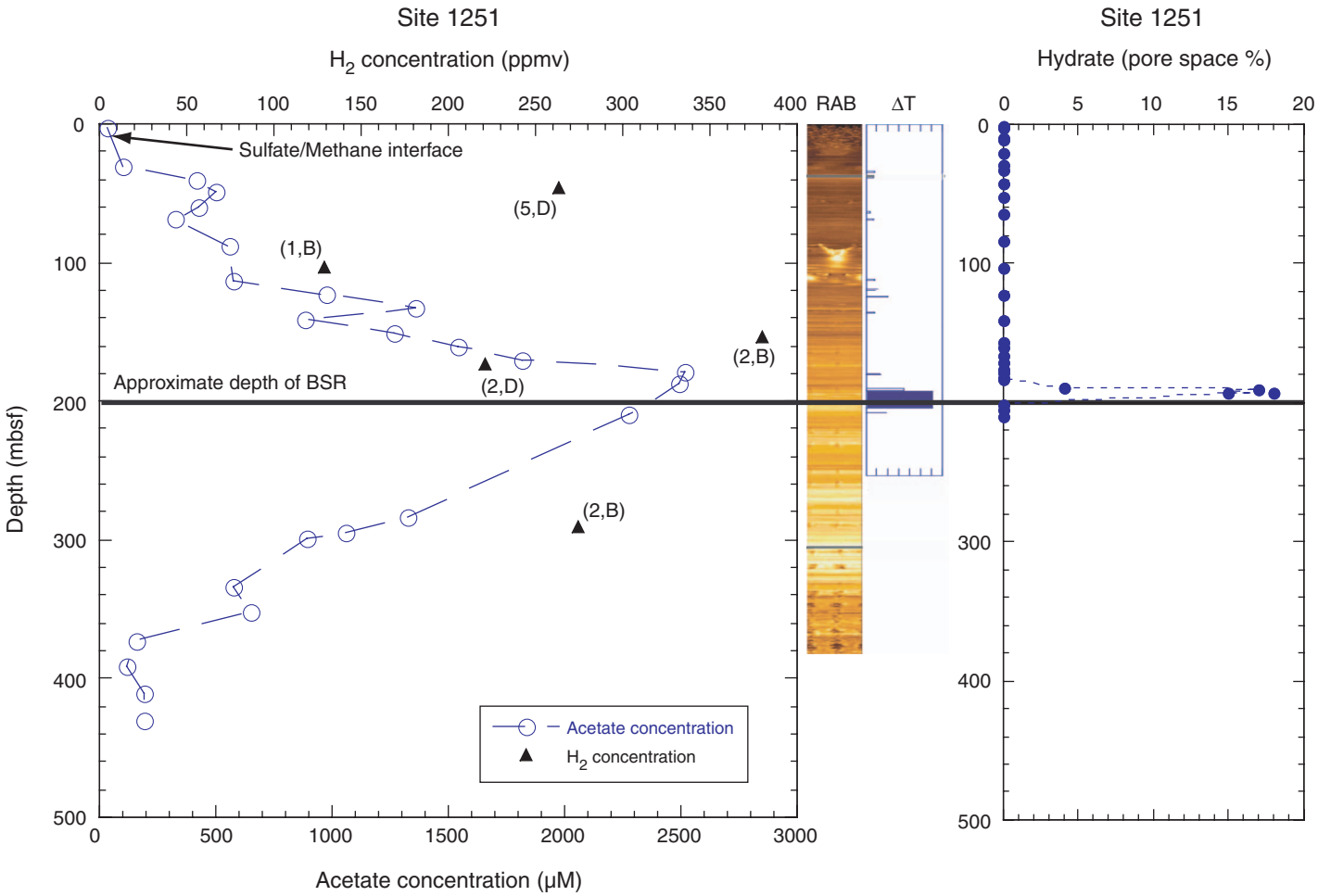

Figure F8. Plot of acetate ion concentration with depth for Site 1252. The panel to the right shows low temperature anomalies recorded by infrared camera scans (blue spikes), which indicate likely areas of gas hydrate decomposition in the recovered core. There is no methanogen or resistivity-at-the-bit (RAB) data for this site. Note the general correspondence of higher concentrations of acetate with gas hydrate accumulations, the bottom-simulating reflector (BSR), and a buildup below the BSR with low concentrations of methanogens. The overall increase in acetate concentration below the BSR may be due to a combination of lithology change and fluid from another system not sampled at the other sites of Leg 204. ΔT = temperature change.

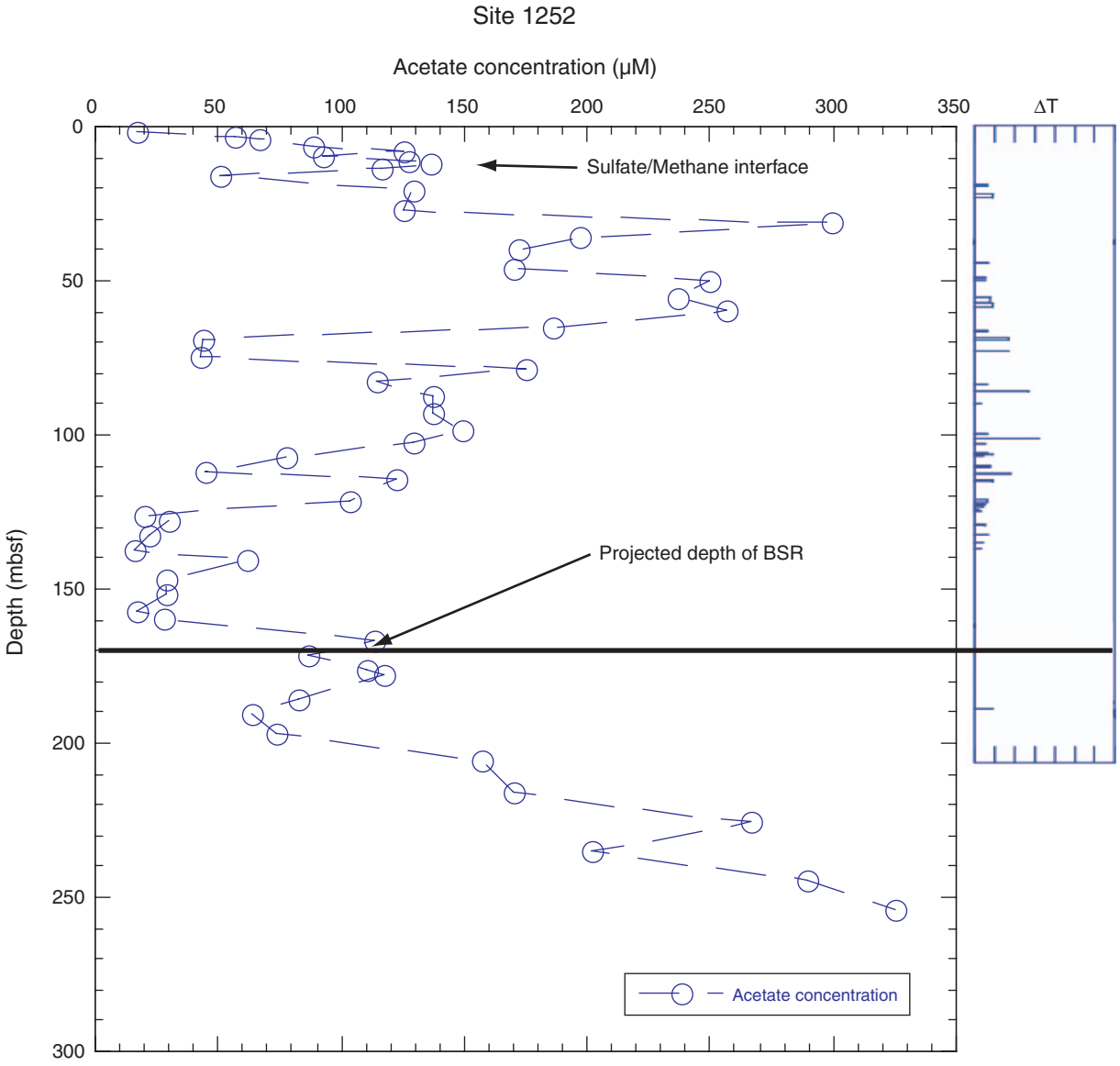

Figure F9. Plot of Leg 204 acetate ion concentration vs. temperature. The lack of any general relationship such as an increase with depth as observed by Wellsbury et al. (1997) at Blake Ridge, offshore the southeastern Atlantic coast of the United States, suggests that acetogenesis by pyrolysis of organic matter during early diagenesis is not occurring here.

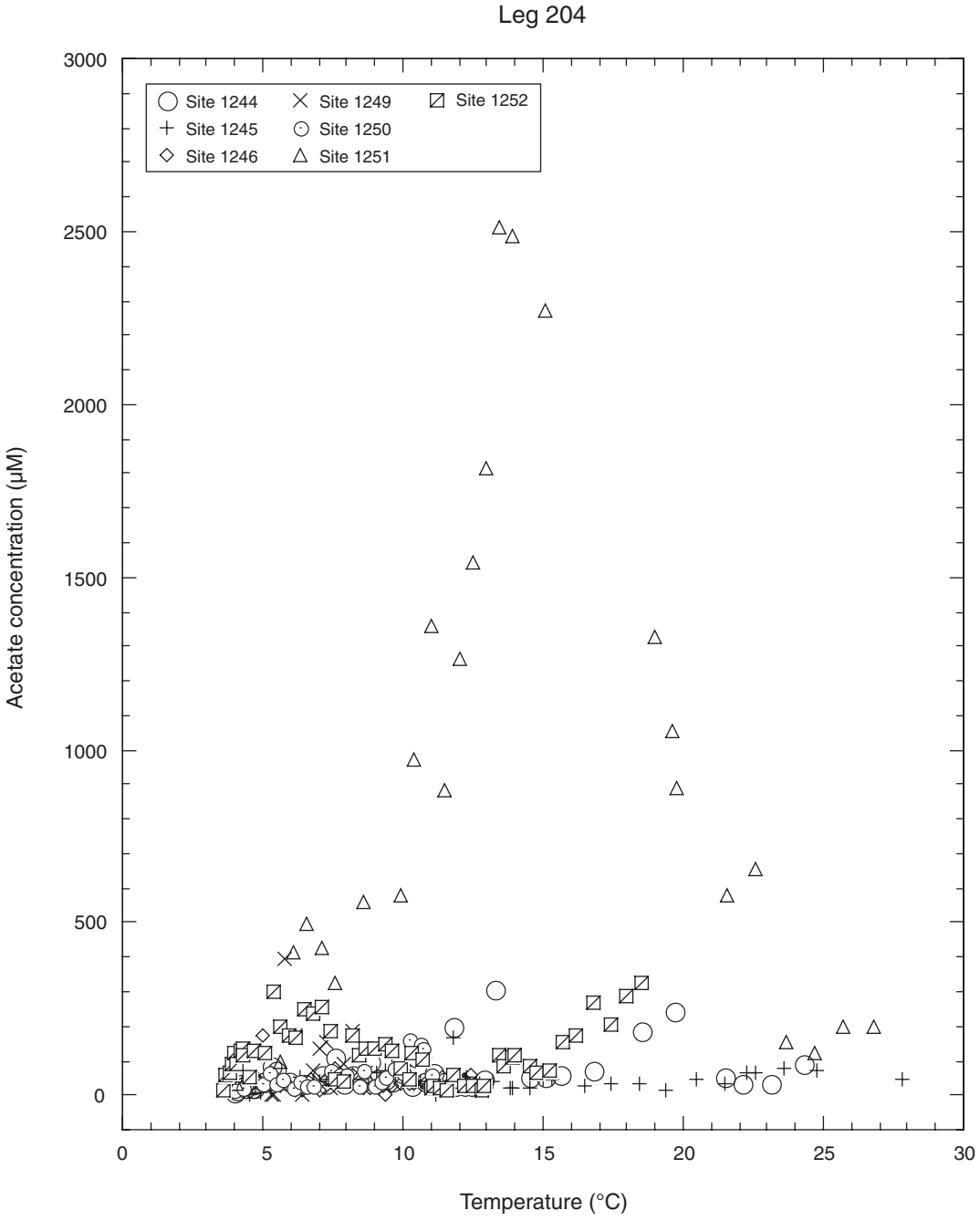

Table T1. Acetate ion concentration in interstitial pore water from Sites 1244, 1245, 1249, 1250, 1251, and 1252. (See table note. Continued on next page.)

Sample ID	Date	Time	Core, section, interval (cm)	Depth (mbsf)	Acetate (μM)
			204-1244C-		
1490216	7/15/2002	17:53	1H-1, 65–75	0.65	10.97
1490227	7/15/2002	17:54	1H-2, 65–75	2.15	12.26
1490239	7/15/2002	17:55	1H-3, 65–75	3.65	34.19
1490204	7/15/2002	17:50	1H-4, 60–70	5.10	28.39
1490250	7/15/2002	17:57	2H-1, 140–150	6.90	20.00
1490260	7/15/2002	17:58	2H-2, 140–150	8.40	43.87
1490272	7/15/2002	17:59	2H-3, 140–150	9.90	19.35
1490283	7/15/2002	18:01	2H-4, 140–150	11.40	22.58
1490293	7/15/2002	18:03	2H-5, 140–150	12.90	33.55
1490303	7/15/2002	18:04	2H-6, 140–150	14.40	32.26
1490401	7/15/2002	19:14	3H-1, 140–150	16.40	43.22
1490431	7/15/2002	19:20	3H-5, 140–150	22.40	83.87
1490450	7/15/2002	19:26	3H-7, 84–94	24.84	73.54
1490477	7/15/2002	19:31	4H-5, 135–150	31.85	41.29
1490500	7/15/2002	19:55	5H-5, 135–150	41.35	33.55
1490521	7/15/2002	19:59	6H-5, 135–150	50.71	57.42
1490532	7/15/2002	20:01	7H-2, 135–150	54.79	34.46
1490542	7/15/2002	20:03	7H-5, 135–150	58.97	110.96
1490552	7/15/2002	20:05	8H-2, 135–150	64.37	35.82
1490563	7/15/2002	20:09	8H-5, 135–150	68.87	58.06
1490575	7/15/2002	20:10	9H-2, 135–150	74.85	47.61
1490586	7/15/2002	20:12	9H-5, 135–150	79.35	94.83
1490597	7/15/2002	20:15	10H-2, 55–70	83.55	43.53
1490608	7/15/2002	20:16	10H-5, 135–150	88.38	44.51
1490620	7/15/2002	20:17	11H-2, 135–150	93.08	38.09
1490631	7/15/2002	20:19	11H-5, 135–150	97.58	65.80
1490642	7/15/2002	20:25	12H-2, 135–150	103.35	27.21
1490653	7/15/2002	20:27	12H-5, 135–150	107.85	110.32
1490664	7/15/2002	20:28	13H-2, 135–150	112.85	42.62
1490674	7/15/2002	20:29	13H-5, 135–150	117.35	68.38
1490686	7/15/2002	20:31	15H-2, 135–150	123.85	42.62
1490696	7/15/2002	20:32	15H-5, 135–150	128.35	201.28
1490720	7/15/2002	20:35	19X-2, 135–150	145.85	46.45
1490740	7/15/2002	20:39	20X-3, 135–150	153.55	309.66
1490838	7/16/2002	15:03	22X-3, 135–150	172.65	54.19
1491398	7/16/2002	20:05	23X-3, 135–150	182.25	50.33
1491221	7/16/2002	18:26	24X-3, 135–150	191.45	56.13
1491244	7/16/2002	19:40	26X-3, 135–150	210.45	72.25
1491277	7/16/2002	19:45	29X-3, 130–150	238.56	186.44
1491299	7/16/2002	19:47	31X-3, 130–150	258.60	245.79
1491332	7/16/2002	19:52	34X-3, 130–150	287.60	50.96
1491343	7/16/2002	19:54	35X-3, 130–150	297.33	36.77
1491365	7/16/2002	19:58	37X-1, 130–150	313.50	34.19
1491387	7/16/2002	20:00	39X-1, 130–150	332.80	91.61
			204-1245B-		
1501290	8/6/2002	18:16	1H-5, 140–150	7.40	CI
1501340	8/6/2002	19:09	2H-4, 140–150	15.40	7.10
1501385	8/6/2002	20:53	3H-2, 140–150	21.90	17.42
1501433	8/6/2002	21:41	4H-2, 140–150	31.40	37.42
1501483	8/6/2002	22:41	5H-2, 140–150	40.90	50.32
1501559	8/6/2002	23:17	6H-2, 140–150	50.40	43.22
1501639	8/6/2002	23:45	6H-5, 78–88	54.28	39.35
1501707	8/7/2002	01:56	7H-2, 140–150	58.95	47.74
1501800	8/7/2002	03:24	8H-2, 132–142	69.32	54.84
1501819	8/7/2002	03:42	8H-4, 140–150	72.32	39.35
1502067	8/7/2002	05:25	9H-4, 140–150	81.62	48.38
1501934	8/7/2002	05:14	10H-5, 140–150	92.53	65.80
1501953	8/7/2002	05:14	11H-2, 140–150	97.37	69.83
1501972	8/7/2002	05:15	11H-5, 140–150	101.87	119.35
1501991	8/7/2002	05:16	12H-2, 140–150	107.37	63.94
1502010	8/7/2002	05:17	12H-5, 140–150	111.87	87.09
1502029	8/7/2002	05:19	13H-2, 111–126	116.61	41.72
1502048	8/7/2002	05:19	13H-5, 104–119	120.80	41.93
1502184	8/7/2002	08:50	14H-1, 125–140	123.95	111.55
1502203	8/7/2002	08:51	14H-2, 135–150	125.45	36.13
1502222	8/7/2002	08:52	15X-3, 130–150	130.66	CI
1502271	8/7/2002	11:10	16X-3, 130–150	141.80	164.51
1502294	8/7/2002	12:37	18X-2, 113–138	151.73	51.24
1502355	8/7/2002	13:48	19X-2, 125–150	159.75	32.90
1502455	8/7/2002	15:16	20X-2, 125–150	169.25	38.54
1502560	8/7/2002	16:57	21X-2, 117–142	178.77	22.58
1502579	8/7/2002	17:03	21X-4, 7–102	181.27	21.77
1502620	8/7/2002	17:53	22X-5, 125–150	192.65	23.87
1502675	8/7/2002	18:52	23X-5, 125–150	201.95	48.97
1502724	8/7/2002	19:51	24X-2, 125–150	206.95	45.80
1502817	8/7/2002	21:33	26X-5, 75–100	230.33	26.45
1502967	8/8/2002	00:46	28X-2, 125–150	245.68	34.84
1503099	8/8/2002	03:37	30X-2, 125–150	264.95	35.48
1503261	8/8/2002	06:36	32X-2, 125–150	284.25	18.06
1503360	8/8/2002	12:17	35X-2, 125–150	303.55	49.03
1503478	8/8/2002	14:40	37X-2, 125–150	322.75	30.97
1503550	8/8/2002	16:15	38X-5, 125–150	336.95	63.87
1503592	8/8/2002	18:05	39X-2, 125–150	341.95	63.87
1503697	8/8/2002	21:43	41X-2, 125–150	361.25	78.70
1503838	8/9/2002	01:10	43X-4, 125–150	383.55	70.96
1504206	8/9/2002	15:37	50X-2, 125–150	438.27	47.09
			204-1246B-		
1505657	8/11/2002	17:43	2H-2, 145–150	7.65	173.67
1505676	8/11/2002	17:44	2H-5, 145–150	12.15	64.39
1505705	8/11/2002	18:39	3H-2, 140–150	17.10	27.66
1505724	8/11/2002	18:40	3H-5, 140–150	21.60	26.30
1505752	8/11/2002	19:27	4H-2, 140–150	26.60	15.42
1505771	8/11/2002	19:28	4H-5, 140–150	31.10	14.51
1505790	8/11/2002	19:31	5H-2, 140–150	36.10	49.43
1505809	8/11/2002	19:33	5H-5, 140–150	40.60	15.87
1505828	8/11/2002	19:35	6H-2, 140–150	45.57	43.98
1505847	8/11/2002	19:36	6H-5, 140–150	50.00	78.45
1505866	8/11/2002	19:41	7H-2, 140–150	54.99	35.37
1505885	8/11/2002	19:43	7H-5, 140–150	59.49	56.23
1505919	8/11/2002	21:14	8H-2, 140–150	64.60	34.01
1506114	8/12/2002	00:16	8H-4, 0–25	66.20	22.67
1505938	8/11/2002	21:16	8H-5, 140–150	69.10	22.67
1505957	8/11/2002	21:18	9H-2, 140–150	73.81	26.30
1505976	8/11/2002	21:20	9H-5, 140–150	78.31	24.49
1505997	8/11/2002	21:21	9H-7, 52–68	79.93	3.17
1506063	8/11/2002	23:09	10H-2, 140–150	83.60	26.30
1506082	8/11/2002	23:11	10H-5, 132–142	88.02	35.82
1506025	8/11/2002	23:03	11H-2, 140–150	93.10	33.10
1506044	8/11/2002	23:05	11H-5, 83–93	96.55	33.10
1506143	8/12/2002	02:00	12H-2, 140–150	102.60	30.83
1506162	8/12/2002	02:02	12H-4, 67–87	104.73	29.93
1506181	8/12/2002	02:05	12H-5, 0–20	105.33	37.18
1506219	8/12/2002	02:09	13H-2, 135–150	112.05	50.33
1506257	8/12/2002	02:12	14H-2, 135–150	121.55	47.61
1506276	8/12/2002	02:14	15H-2, 140–150	125.15	47.16
1506295	8/12/2002	02:15	15H-4, 140–150	128.15	57.14
1506349	8/12/2002	07:02	16H-2, 140–150	132.70	33.56
			204-1249C-		
1492826	7/26/2002	02:44	1H-1, 110–125	1.10	49.67
1492846	7/26/2002	02:57	2H-2, 0–30	3.40	42.62
1492884	7/26/2002	05:58	3H-1, 74–89	5.74	25.80
1492904	7/26/2002	06:00	3H-2, 41–51	6.96	26.75
1492930	7/26/2002	07:32	4H-2, 44–62	15.77	CI
1492957	7/26/2002	07:35	4H-5, 86–101	17.61	CI
1492978	7/26/2002	07:36	5H-2, 20–25	25.70	392.23
1493057	7/26/2002	09:25	7H-1, 71–86	35.71	176.39
1493078	7/26/2002	09:27	7H-5, 76–91	38.89	CI
1493107	7/26/2002	10:19	8H-3, 18–33	47.64	74.82
1493128	7/26/2002	10:21	8H-4, 124–139	50.18	136.12
1493174	7/26/2002	11:25	9H-2, 133–148	56.83	155.47
1493202	7/26/2002	11:27	9H-3, 120–135	58.18	23.13
1493228	7/26/2002	13:07	11H-4, 104–119	69.17	89.67
1493248	7/26/2002	13:09	11H-6, 95–115	71.87	54.41

Table T1 (continued).

Sample ID	Date	Time	Core, section, interval (cm)	Depth (mbsf)	Acetate (μM)
1493281	7/26/2002	14:26	12H-1, 120–140	75.70	187.73
1493326	7/26/2002	15:13	13H-2, 79–99	86.29	66.20
			204-1250C-		
1498856	8/2/2002	22:49	1H-1, 0–10	0.00	11.79
1498927	8/3/2002	00:25	2H-CC, 10–15	5.16	19.50
1498970	8/3/2002	01:16	3H-2, 140–150	16.90	31.74
1499005	8/3/2002	01:18	3H-5, 140–150	21.40	63.94
1499078	8/3/2002	02:41	4H-2, 140–150	26.40	30.83
1499097	8/3/2002	02:42	4H-4, 140–150	29.00	48.97
1499155	8/3/2002	03:40	5H-2, 140–150	35.88	23.13
1499174	8/3/2002	03:41	5H-5, 133–143	40.31	37.64
1499199	8/3/2002	04:47	6H-2, 57–67	44.57	25.39
1499218	8/3/2002	04:49	6H-5, 118–128	48.95	25.85
1499285	8/3/2002	06:25	7H-5, 130–140	58.00	69.83
1499328	8/3/2002	07:22	8H-2, 140–150	64.40	60.76
1499309	8/3/2002	06:57	8H-5, 140–150	68.90	58.04
1499437	8/3/2002	10:40	10H-2, 81–96	75.31	28.57
1499418	8/3/2002	10:35	10H-5, 135–150	79.81	71.65
1499516	8/3/2002	13:45	11H-3, 95–110	86.36	25.39
1499536	8/3/2002	13:45	11H-5, 130–145	89.31	38.54
1499564	8/3/2002	14:41	12H-1, 50–65	92.50	55.32
1499583	8/3/2002	14:42	12H-5, 140–155	98.43	79.81
1499616	8/3/2002	15:45	13H-2, 130–150	103.19	68.47
1499635	8/3/2002	15:46	13H-5, 130–150	107.69	158.71
1499689	8/3/2002	16:53	14H-2, 130–150	113.80	150.55
1499708	8/3/2002	16:54	14H-4, 40–60	115.33	135.58
1499774	8/3/2002	18:29	15H-1, 106–126	121.56	58.50
1499793	8/3/2002	18:30	15H-4, 100–120	125.86	29.93
1499837	8/3/2002	19:40	17H-1, 130–150	133.30	22.22
1499818	8/3/2002	19:24	17H-3, 130–150	136.30	22.22
1499915	8/3/2002	23:00	19X-2, 130–150	141.30	19.05
1499955	8/3/2002	23:19	19X-5, 130–150	145.75	21.31
			204-1251B-		
1493592	7/27/2002	02:13	1H-2, 145–150	2.95	34.19
1493686	7/27/2002	04:52	4H-2, 140–150	31.00	98.70
1493736	7/27/2002	05:32	5H-2, 131–141	40.41	415.46
1493796	7/27/2002	06:44	6H-2, 130–140	49.22	496.74
1493921	7/27/2002	08:08	7H-2, 140–150	59.50	424.49
1493961	7/27/2002	08:09	8H-2, 140–150	69.00	327.08
1494032	7/27/2002	09:08	10H-2, 140–150	88.00	559.32
1494269	7/27/2002	18:18	13H-5, 130–150	112.85	578.67
1494367	7/27/2002	19:56	14H-5, 130–150	122.41	972.20
1494440	7/27/2002	21:01	15H-5, 124–144	132.34	1358.62
1494534	7/27/2002	22:47	16H-5, 121–141	141.81	883.17
1494632	7/28/2002	00:19	17H-5, 80–100	150.90	1266.37
1494696	7/28/2002	02:08	19H-4, 130–150	161.09	1545.06
1494772	7/28/2002	03:21	20H-5, 130–150	170.48	1817.95
1494841	7/28/2002	05:01	22H-4, 128–148	178.48	2515.32
1494914	7/28/2002	06:39	23H-4, 102–122	187.72	2488.87
1494985	7/28/2002	08:51	26X-4, 130–150	209.88	2272.11
1495410	7/28/2002	20:20	34X-2, 128–148	283.78	1324.43
1495526	7/28/2002	23:56	36X-2, 130–150	295.40	1056.71
1495564	7/28/2002	23:59	36X-5, 80–100	299.40	890.27
1495797	7/29/2002	08:45	41X-2, 130–150	333.40	578.03
1495879	7/29/2002	10:47	43X-2, 130–150	351.60	653.51
1495944	7/29/2002	14:11	45X-3, 130–150	372.30	155.47
1496030	7/29/2002	16:59	47X-3, 130–150	391.60	119.99
1496203	7/29/2002	23:44	50X-3, 130–150	410.80	196.12
1496350	7/30/2002	03:41	52X-3, 130–150	430.10	196.12
			204-1252A-		
1512133	8/30/2002	11:04	1H-1, 135–150	1.35	17.23
1512153	8/30/2002	11:06	1H-2, 135–150	2.85	56.68
1512173	8/30/2002	11:07	1H-3, 85–100	3.85	66.20
1512207	8/30/2002	12:03	2H-1, 135–150	6.25	88.88
1512227	8/30/2002	12:03	2H-2, 135–150	7.75	125.15
1512247	8/30/2002	12:05	2H-3, 135–150	9.25	92.50
1512267	8/30/2002	12:06	2H-4, 135–150	10.75	127.42
1512287	8/30/2002	12:07	2H-5, 135–150	12.25	136.04
1512307	8/30/2002	12:07	2H-6, 135–150	13.75	116.08
1512343	8/30/2002	14:55	3H-2, 135–150	16.00	50.33
1512363	8/30/2002	14:56	3H-5, 135–150	20.50	129.69
1512383	8/30/2002	14:57	4H-2, 135–150	26.75	125.61
1512403	8/30/2002	14:58	4H-5, 135–150	31.13	298.83
1512432	8/30/2002	16:11	5H-2, 135–150	35.34	197.25
1512452	8/30/2002	16:12	5H-5, 135–150	39.84	171.86
1512496	8/30/2002	16:52	6H-2, 135–150	45.75	170.04
1512516	8/30/2002	16:53	6H-5, 135–150	50.25	249.40
1512536	8/30/2002	16:54	7H-2, 135–150	55.25	236.70
1512556	8/30/2002	16:55	7H-5, 135–150	59.75	256.20
1512649	8/30/2002	18:44	8H-2, 135–150	64.75	185.92
1512669	8/30/2002	18:45	8H-5, 135–150	69.25	43.98
1512689	8/30/2002	18:46	9H-2, 135–150	74.25	43.08
1512709	8/30/2002	18:47	9H-5, 135–150	78.75	175.49
1512791	8/30/2002	20:49	10H-2, 45–60	82.85	114.72
1512811	8/30/2002	20:51	10H-5, 135–150	87.35	136.94
1512831	8/30/2002	20:53	11H-2, 135–150	93.25	136.94
1513110	8/31/2002	00:41	11H-6, 80–95	98.70	149.19
1512871	8/30/2002	20:59	12H-2, 135–150	102.75	128.78
1512891	8/30/2002	21:01	12H-5, 135–150	107.15	77.99
1512911	8/30/2002	21:03	13H-2, 135–150	112.25	44.44
1512770	8/30/2002	20:39	13H-4, 67–87	114.57	121.98
1512931	8/30/2002	21:04	14H-2, 135–150	121.75	103.84
1512951	8/30/2002	21:06	14H-5, 102–127	125.84	19.50
1513187	8/31/2002	03:33	15X-2, 135–150	127.85	29.47
1513210	8/31/2002	03:35	15X-5, 130–150	132.18	22.22
1513256	8/31/2002	05:03	16X-2, 130–150	137.50	15.42
1513279	8/31/2002	05:28	16X-4, 130–150	140.50	61.22
1513299	8/31/2002	05:36	17X-2, 130–150	147.20	29.02
1513319	8/31/2002	05:41	17X-5, 120–140	151.60	28.57
1513362	8/31/2002	06:48	18X-2, 130–150	156.90	16.78
1513382	8/31/2002	06:49	18X-4, 100–120	159.60	28.11
1513428	8/31/2002	07:32	19X-2, 130–150	166.60	113.82
1513448	8/31/2002	07:33	19X-5, 130–150	171.10	86.61
1513468	8/31/2002	07:34	20X-2, 130–150	176.30	110.64
1513488	8/31/2002	07:35	20X-3, 130–150	177.80	117.44
1513508	8/31/2002	07:36	21X-2, 130–150	185.90	82.53
1513528	8/31/2002	07:36	21X-5, 130–150	190.36	63.48
1513582	8/31/2002	11:37	22X-3, 130–150	197.00	73.91
1513602	8/31/2002	11:38	23X-3, 130–150	205.78	157.35
1513643	8/31/2002	12:12	24X-3, 130–150	215.50	170.50
1513663	8/31/2002	12:13	25X-3, 130–150	225.20	266.63
1513701	8/31/2002	12:14	26X-3, 130–150	234.80	202.24
1513721	8/31/2002	12:15	27X-3, 130–150	244.50	288.85
1513741	8/31/2002	12:15	28X-3, 130–150	254.14	324.67

Note: CI = chromatographic interference, acetate retention time obscured by large peak.

Table T2. Hydrogen, helium, and methane gas concentrations in PCS gas samples.

Core	Sample	Volume (mL) Start	Volume (mL) Stop	Depth (mbsf)	H_2 (ppm)	Average H_2 (ppm)	He (ppm)	CH_4 (%)
204-1244E-								
11P	G14	134	110	72.6	595.00	595.00	5.80	99.94
15P	G6	125	195	103.1	1035.52	1035.52	38.20	99.89
15P	G8	120	90	103.0	794.82	915.17	14.13	99.92
204-1249F-								
4P	G12	140	105	13.5	173.40		2.51	99.98
4P	G18	130	100	13.5	64.93		2.37	99.99
4P	G20	140	103	13.5	62.48		2.15	99.99
4P	G24	140	103	13.5	67.26		2.12	99.99
4P	G26	138	110	13.5	105.07		2.13	99.99
4P	G38	130	95	13.5	105.64	96.46	2.24	99.99
204-1249C-								
6P	G3	140	105	33.5	16.45		2.30	100.00
6P	G5	140	105	33.5	20.27		2.34	100.00
6P	G8	140	115	33.5	18.04	18.39	2.35	100.00
204-1249F-								
6P	G10	140	103	33.5	18.81	18.81	2.23	100.00
14P	G5	135	105	72.4	74.56		5.36	99.99
14P	G5	135	105	72.4	85.41	79.98	ND	99.99
204-1250D-								
5P	G3	134	100	35.0	250.40		17.17	99.97
5P	G8	135	100	35.0	317.95	284.17	7.90	99.97
204-1250C-								
9P	G2	152	115	71.0	66.11		9.02	99.99
9P	G5	110	85	71.0	108.52		31.63	99.99
9P	G6	140	110	71.0	139.38	122.69	19.55	99.98
204-1250D-								
13P	G6	130	100	103.5	120.15		21.77	99.99
13P	G7	125	105	103.5	119.65		8.21	99.99
13P	G7	125	105	103.5	133.68	126.66	53.63	99.98
204-1251D-								
6P	G2	135	100	45.9	490.36		ND	99.95
6P	G3	125	90	45.9	282.65		8.91	99.97
6P	G5	138	100	45.9	154.26		9.49	99.98
GP	G6	135		45.9	215.80		2.56	99.98
SP	G10	120	90	45.9	176.53	263.92	7.77	99.98
204-1251B-								
12P	G4	140	105	104.1	128.75	128.75	29.09	99.98
18P	G6	145	100	153.4	379.92		29.29	99.96
18P	G7	130	99	153.4	379.10	379.51	23.45	99.96
204-1251D-								
21P	G2	140	103	173.4	215.28		58.08	99.97
21P	G5	135	100	173.4	227.48	221.38	ND	99.98
204-1251B-								
35P	G2	135	100	290.6	209.13		7.24	99.98
35P	G9	137	105	290.6	339.06	274.10	21.80	99.96

Notes: Hydrogen concentrations varied widely between gas samples taken from the same core over time. There is some systematic variation with time such that the later samples tend to have higher concentrations that likely reflect the high solubility of hydrogen. Because gas from the core must travel through water to be sampled, earlier samples reflect residual hydrogen. Later, when the water is more saturated with hydrogen content, gaseous concentration should increase. Average hydrogen concentrations are given and plotted in Figures **F3,** p. 11, **F4,** p. 12, **F5,** p. 13, **F6,** p. 14, **F7,** p. 15, and **F8,** p. 16, in order to compensate for this sampling artifact. Sample start and stop volumes note the amount of gas sampled (e.g., 145–100 equates to 45 mL gas in the sample). ND = none detected.